Anal. Chem. **2010,** *82,* 5892–5896

Enhanced Solid-State Electrochemiluminescence of Tris(2,2′-bipyridyl)ruthenium(II) Incorporated into Electrospun Nanofibrous Mat

Dan Shan,*,† Bo Qian,† Shou-Nian Ding,*,‡ Wei Zhu,‡ Serge Cosnier,§ and Huai-Guo Xue†

Key Laboratory of Environmental Materials & Environmental Engineering of Jiangsu Province, College of Chemistry & Chemical Engineering, Yangzhou University, Yangzhou 225002, China, School of Chemistry & Chemical Engineering, Southeast University, Nanjing 211189, China, and Département de Chimie Moléculaire UMR-5250, ICMG FR-2607, CNRS Université Joseph Fourier, BP-53, 38041 Grenoble, France

An electrospun poly(acrylonitrile-*co*-acrylic acid) nanofiber mat (PAN-*co*-PAA_{nfm}) was successfully collected on the surface of a glassy carbon electrode (GCE). Scanning electron microscope (SEM) images showed that the porous electrospun mat was composed of ∼160 nm diameter of uniform knitted nanofibers. The cationic luminescence probe, tris(2,2′-bipyridyl)ruthenium(II) complex ($[Ru(bpy)_3]^{2+}$), was innovatively and first incorporated into the negatively charged PAN-*co*-PAA_{nfm}-modified GCE via electrostatic interaction. Compared with the $[Ru(bpy)_3]^{2+}$ immobilized on normal PAN-*co*-PAA deposited coating, $[Ru(bpy)_3]^{2+}$/PAN-*co*-PAA_{nfm} exhibited dramatically enhanced electrochemical and electrochemiluminescence (ECL) performances, namely, more than 100 times higher ECL intensity could be feasibly obtained via the electrospinning technique.

The development of simple, reliable, and controllable procedures to modify an electrode continues to receive considerable attention, since it is a key step in the design and fabrication of good performances of electrochemical sensors[1] and electrochemiluminescent sensors.

Immobilization of $[Ru(bpy)_3]^{2+}$ upon the electrode to develop solid-state ECL sensors is always attractive due to the following factors: (1) $[Ru(bpy)_3]^{2+}$ intrinsic properties such as chemical stability, reversible electrochemical behavior, and high luminescent quantum yield; (2) regenerated ECL sensors for chemical, biochemical, and clinical analysis; (3) solid-state ECL detectors for combining with high-performance liquid chromatography, capillary electrophoresis, and microchip electrophoresis to save luminescent reagent and improve separation efficiency.[2,3]

Until now, many different methods and materials have been developed to immobilize $[Ru(bpy)_3]^{2+}$.[4] Although some progress has been made in this field, new immobilization methods and materials are still needed to make robust, novel, sensitive, and highly efficient solid-state ECL sensors.

Recently, the electrospinning method has been actively explored. Because of the simplicity of the process, it offers ultrafine polymer fibers with a highly specific surface area and the possibility of various further modifications.[5] When the electric force on induced charges on the polymer liquid overcomes surface tension, a thin polymer jet is ejected. The charged jet is elongated and accelerated by the electric field, undergoes a variety of instabilities, dries, and is deposited on a substrate as a random nanofiber mat. Such nanofibrous mats can be used for a broad range of applications such as filtration,[6] tissue engineering,[7] sensors,[8] solar cells,[9] catalysis,[10] and so on.

Herein we provided another successful example to demonstrate that the electrospinning technique could be efficiently used to develop highly efficient solid-state ECL sensors. We collected electrospun PAN-*co*-PAA_{nfm} on the surface of the GCE. The electrospun PAN-*co*-PAA_{nfm} obtained was first used as a host matrix for $[Ru(bpy)_3]^{2+}$ loading because of their high surface area and the electrostatic interaction of carboxyl anions and $[Ru(bpy)_3]^{2+}$ cations. To ascertain the role of nanofibers in the enhancement of electrode-performance, another $[Ru(bpy)_3]^{2+}$-electrode was fabricated as a reference electrode based on PAN-*co*-PAA normal deposited coating. Dramatically enhanced electrochemical and ECL properties were obtained at the $[Ru(bpy)_3]^{2+}$/PAN-*co*-PAA_{nfm} modified electrode.

EXPERIMENTAL SECTION

Materials. $[Ru(bpy)_3]^{2+}$ and TPA were from Aldrich. Tetracycline, ofloxacin, gentamycin sulfate, L-proline, and NADH

* To whom correspondence should be addressed. E-mail, danshan@yzu.edu.cn; fax, 0086-514-87975244 (D.S.). E-mail, snding@seu.edu.cn; fax, 0086-25-52090621 (S.-N.D.).

† Yangzhou University.

‡ Southeast University.

§ CNRS Université Joseph Fourier.

(1) Cosnier, S. *Appl. Biochem. Biotechnol.* **2000**, *89*, 127–138.
(2) Ding, S. N.; Xu, J. J.; Chen, H. Y. *Electrophoresis* **2005**, *26*, 1737–1744.
(3) Ding, S. N.; Xu, J. J.; Chen, H. Y. *Talanta* **2006**, *70*, 572–577.
(4) Wei, H.; Wang, E. K. *Trends Anal. Chem.* **2008**, *25*, 447–459.
(5) Dzenis, Y. *Science* **2004**, *304*, 1917–1919.
(6) Shin, C. *J. Colloid Interface Sci.* **2006**, *302*, 267–271.
(7) Zhang, Y. Z.; Feng, Y.; Huang, Z. M.; Ramakrishna, S.; Lim, C. T. *Nanotechnology* **2006**, *17*, 901–908.
(8) Wang, Z. G.; Wang, Y.; Xu, H.; Li, G.; Xu, Z. K. *J. Phys. Chem. C* **2009**, *113*, 2955–2960.
(9) Onozuka, K.; Ding, B.; Tsuge, Y.; Naka, T.; Yamazaki, M.; Sugi, S.; Ohno, S.; Yoshikawa, M.; Shiratori, S. *Nanotechnology* **2006**, *17*, 1026–1031.
(10) Yang, G. C.; Gong, J.; Yang, R.; Guo, H. W.; Wang, Y. Z.; Liu, B. F.; Dong, S. J. *Electrochem. Commun.* **2006**, *8*, 790–796.

10.1021/ac100435z
Published on Web 06/15/2010

were obtained from Shanghai Reagent Company (China) and were used as received without further purification. Copolymer PAN-*co*-PAA with a viscosity averaged molecular weight (M_v) of 48 000 g/mol was synthesized following the procedures reported in our previous work.[11,12] Phosphate buffer solution (PBS) was 0.1 M Na_2HPO_4 and NaH_2PO_4, and its pH was adjusted with H_3PO_4 or NaOH solutions. Twice-distilled water was used throughout the experiment.

Apparatus. Electrochemical measurements were performed on a CHI 760C electrochemical workstation with a three-electrode system comprised of a platinum wire as the auxiliary electrode, a saturated electrode (SCE) as the reference electrode, and the glassy carbon disk electrode (GCE) with a diameter of 3 mm as the working electrode. ECL was conducted by a homemade ECL system as described in our previous work,[13] including the CHI 760C electrochemical workstation, a quartz glass electrochemical cell (homemade), a model 1P21 photomultiplier tube (PMT) (Beijing, China), a model GD-1 luminometer (Xi'an, China), and a computer. During measurement, the potential was applied to the working electrode via the electrochemical working station, and ECL was generated. ECL intensities were measured through the bottom of the quartz glass electrochemical cell, which was placed in front of the PMT biased at −600 V. The output current of the PMT was amplified by the luminometer and was recorded through a 1 kΩ resister to the second WE port of the CHI 760C with "scan" choice. Micrographs were obtained with a XL-30E scanning electron microscope (SEM). UV−vis measurements were carried out by using a UV-2550 spectrophotometer. Also, sample films for UV−vis measurements were prepared by incorporating $[Ru(bpy)_3]^{2+}$ in a PAN-*co*-PAA and PAN-*co*-PAA_{nfm} modified platinum gauze electrode with 80 mesh.

Preparation of PAN-*co*-PAA_{nfm} and PAN-*co*-PAA Modified Electrodes. PAN-*co*-PAA was dissolved in DMF to obtain a 13% yellow suspension. The mixture was stirred to a homogeneous solution at room temperature. Electrospinning was carried out with use of a syringe with a 1.2 mm diameter stainless steel spinneret with an inner diameter of 0.7 mm and at an applied electrical potential difference of 15 kV over a 15 cm gap between the spinneret and the GCE surface. A microinfusion pump was set to deliver the solution at a feed rate of 1.0 mL/h with use of a 20 mL syringe leading to a volume of nanofibers of 42 μL. The electrospinning setup is schematically shown in Figure 1, in which the electrode was connected to the ground. The ambient temperature and relative humidity for electrospinning were kept at 25 °C and 40%, respectively. It took 150 s to deposit the nanofibrous mat on the surface of the electrode. The as-prepared electrode was denoted as PAN-*co*-PAA_{nfm}/GCE.

To make a comprehensive study, another electrode based on the PAN-*co*-PAA normal dropping coating was fabricated. Taking into account that the deposition of the same amount of PAN-*co*-PAA than that (42 μL) used to produce nanofibers, totally passivates the electrode, only 2 μL of PAN-*co*-PAA/DMF (13%) was directly spread on the surface of GCE and dried at ambient temperature. This prepared electrode was denoted as PAN-*co*-PAA/GCE.

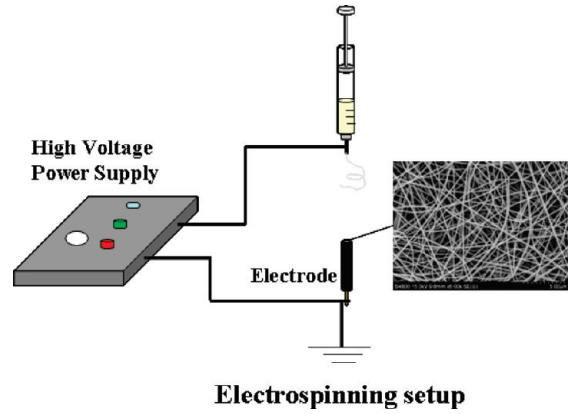

Figure 1. Schematic illustration of the preparation of the PAN-*co*-PAA fibrous mat modified electrode by using an electrospinning technique.

Immobilization of $[Ru(bpy)_3]^{2+}$. The previously prepared PAN-*co*-PAA_{nfm}/GCE and PAN-*co*-PAA/GCE were immersed into 5 mM $[Ru(bpy)_3]^{2+}$ solution for 16 h at 25 °C to reach the equilibrium adsorption of $[Ru(bpy)_3]^{2+}$. Before use, the as-prepared $[Ru(bpy)_3]^{2+}$-electrodes were rinsed under stirring for 20 min with buffer solution to remove the $[Ru(bpy)_3]^{2+}$ not firmly immobilized.

RESULTS AND DISCUSSION

SEM. SEM images of a PAN-*co*-PAA film (A) and PAN-*co*-PAA nanofibrous mat (B,C) coated on the surface of GCE were shown in Figure 2. The PAN-*co*-PAA_{nfm} has an entangled nanofiber network (Figure 2B,C). In Figure 1C, the PAN-*co*-PAA nanofibers are almost uniform with the average diameter of 160 nm. Compared with the PAN-*co*-PAA normal film, the entire structure of the PAN-*co*-PAA_{nfm} provides higher apparent surface area and more porous structure. This structure can provide more obtainable reactive sites and easier diffusion channels for reactants, resulting in enhanced electrochemical reactions.[14]

UV−Visible Spectroscopy. To verify that $[Ru(bpy)_3]^{2+}$ was truly incorporated into the PAN-*co*-PAA_{nfm} and PAN-*co*-PAA film, the UV−vis absorbance spectroscopy experiments were performed. Figure 3 shows the spectra of $[Ru(bpy)_3]^{2+}$ aqueous solution (1×10^{-4} M), $[Ru(bpy)_3]^{2+}$/ PAN-*co*-PAA_{nfm} and $[Ru(bpy)_3]^{2+}$/PAN-*co*-PAA on Pt meshwork in PBS (0.1 M, pH 7.0). For the electrostatically immobilized $[Ru(bpy)_3]^{2+}$ (curves b and c in Figure 3), a typical absorption band around 458 nm can be observed, which is almost the same as that of free $[Ru(bpy)_3]^{2+}$ in aqueous solution (curve a in Figure 3). It is worthy to note that the band at 458 nm should be assigned to the characteristic metal-to-ligand electron transfer band of $[Ru(bpy)_3]^{2+}$.[15] These results confirm successful incorporation of $[Ru(bpy)_3]^{2+}$. In addition, the absorbance obtained by $[Ru(bpy)_3]^{2+}$/PAN-*co*-PAA_{nfm} is about 4 times higher than that of $[Ru(bpy)_3]^{2+}$/PAN-*co*-PAA, which indicates the higher loading of $[Ru(bpy)_3]^{2+}$ into PAN-*co*-PAA_{nfm}. In order to more accurately compare the immobilized amount of ruthenium complex, the

(11) Shan, D.; Cheng, G. X.; Zhu, D. B.; Xue, H. G.; Cosnier, S.; Ding, S. N. *Sens. Actuators, B: Chem.* **2009**, *137*, 259–265.
(12) Shan, D.; Wang, S. X.; He, Y. Y.; Xue, H. G. *Mater. Sci. Eng., C* **2008**, *28*, 213–217.
(13) Shan, D.; Ding, S. N.; Xu, J. J.; Zhu, W.; Zhang, T.; Chen, H. Y.; Cosnier, S. *Electrochem. Commun.* **2010**, *12*, 227–230.
(14) Huang, J. *Pure. Appl. Chem.* **2006**, *78*, 15–27.
(15) Miao, W. J.; Bard, A. J. *Anal. Chem.* **2003**, *75*, 5825–5834.

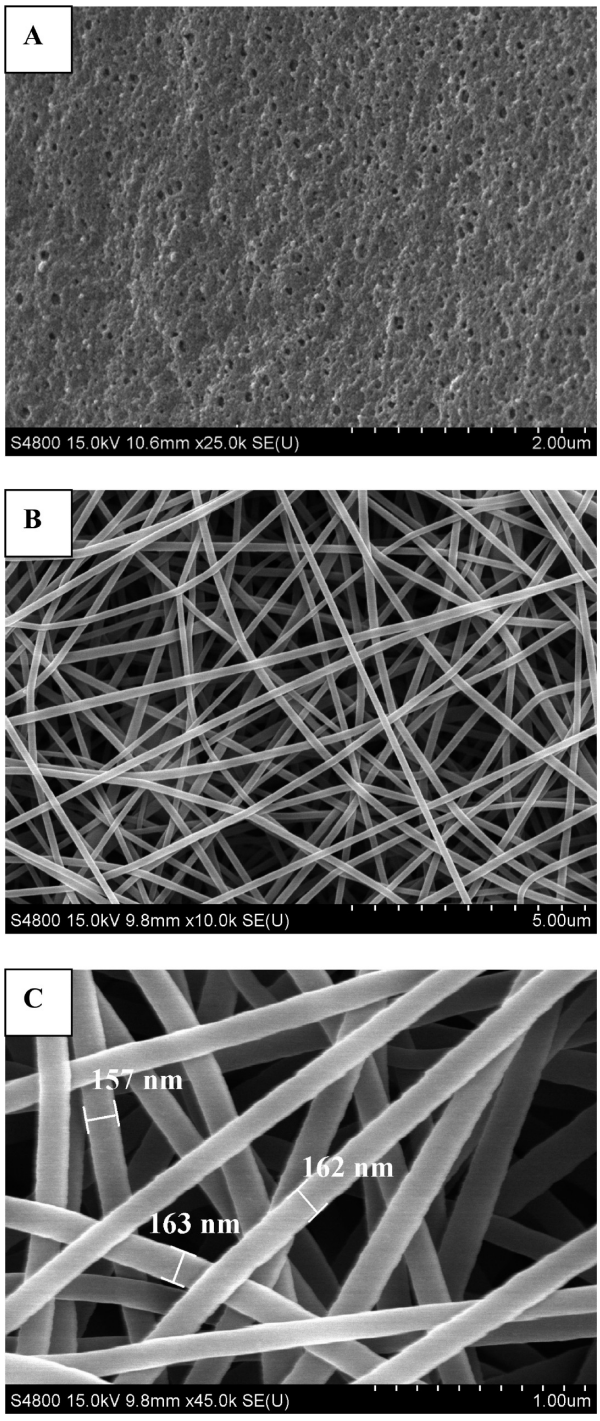

Figure 2. SEM images of PAN-*co*-PAA normal film (A) and PAN-*co*-PAA_{nfm} (B, C) coated on GCE.

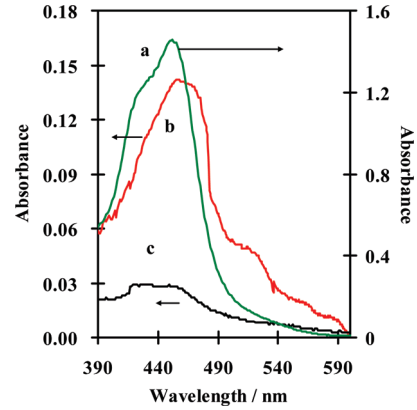

Figure 3. UV−vis spectra for $[Ru(bpy)_3]^{2+}$ in aqueous solutions (a), incorporated in PAN-*co*-PAA_{nfm} (b), and PAN-*co*-PAA coating (c) on the platinum gauze electrode.

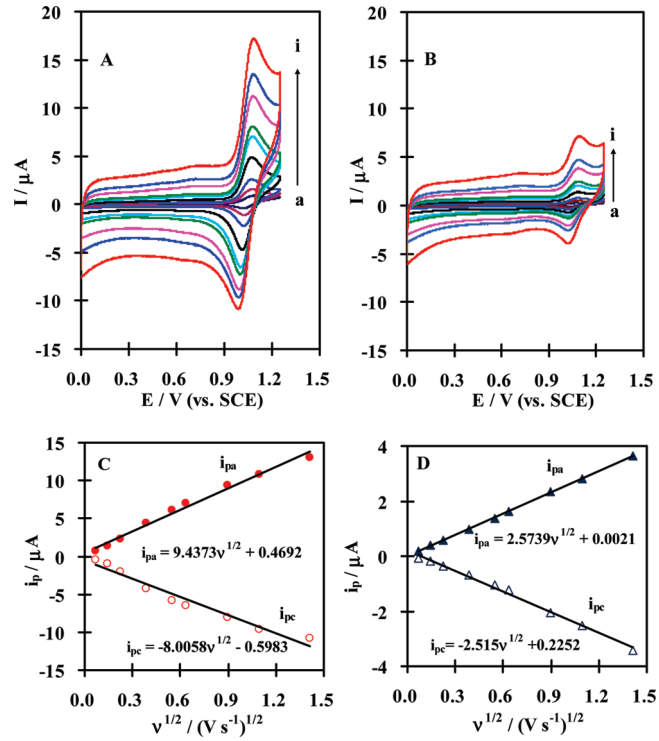

Figure 4. Cyclic voltammograms of $[Ru(bpy)_3]^{2+}$-electrode modified by PAN-*co*-PAA_{nfm} (A) and normal deposited film (B) in 0.1 M PBS (pH 7.0) at different scan rates (from a to i, 5, 20, 50, 150, 300, 400, 800, 1200, 2000 mV s^{-1}, respectively) and relationship between the peak currents and the square roots of the scan rate for the nanofibers mat (C) and normal film (D).

$[Ru(bpy)_3]^{2+}$/PAN-*co*-PAA_{nfm} and $[Ru(bpy)_3]^{2+}$/PAN-*co*-PAA modified electrodes were soaked into DMF to solubilize the polymeric materials. It appears that the $Ru(bpy)_3^{2+}$ solution obtained from the nanofibers presents a 3.7 times higher absorbance than that due to the spread polymer, thus corroborating the preceding result.

Voltammetric Behavior. The electrochemical behaviors of $[Ru(bpy)_3]^{2+}$/PAN-*co*-PAA_{nfm}/GCE and $[Ru(bpy)_3]^{2+}$/PAN-*co*-PAA/GCE were initially investigated using cyclic voltammetry (CV) at different scan rates (Figure 4). The $[Ru(bpy)_3]^{2+}$/PAN-*co*-PAA_{nfm} electrode exhibits an anodic peak potential (E_{pa}) and cathodic peak potential (E_{pc}) at 1.07 and 1.02 V, respectively. Its formal potential $E^{0\prime}$ (defined as the average of E_{pa} and E_{pc}) is 1.04 V, which corresponds to the redox signal of $[Ru(bpy)_3]^{2+/3+}$.[13] E_{pa} and E_{pc} are independent of the scan rate, and the i_{pa}/i_{pc} ratio is 1.17 (theoretically, $i_{pa}/i_{pc} = 1$) for almost all the scan rates, characterizing thus the reversible redox behavior of the $[Ru(bpy)_3]^{2+}$ species immobilized on PAN-*co*-PAA_{nfm}/GCE. Similar characteristics were recorded for the $[Ru(bpy)_3]^{2+}$/PAN-*co*-PAA electrode, namely, a formal potential $E^{0\prime}$ of 1.05 V and an i_{pa}/i_{pc} ratio of 1.02. In contrast, the comparison of the peak intensity of the redox couple clearly

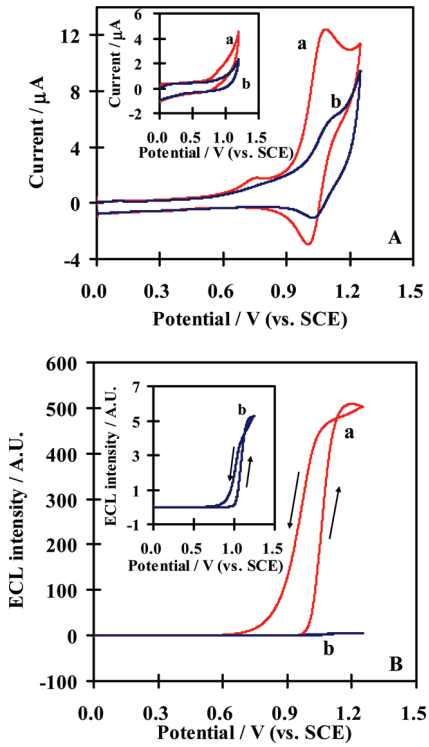

Figure 5. Cyclic voltammograms (A) and corresponding ECL behaviors (B) of $[Ru(bpy)_3]^{2+}$-electrodes modified by PAN-*co*-PAA_{nfm} (a) and normal film (b) in 0.1 M PBS (pH 7.0) containing 1.0×10^{-4} M TPA. Scan rate: 100 mV s^{-1}. The PMT biased at −600 V. Inset of part A: cyclic voltammograms of PAN-*co*-PAA_{nfm}/GCE (a) and PAN-*co*-PAA/GCE (b) in 0.1 M PBS (pH 7.0) containing 0.01 M TPA. Scan rate: 100 mV s^{-1}.

indicates the immobilization of a four time higher amount of $Ru(bpy)_3^{2+}$ for the $[Ru(bpy)_3]^{2+}$/PAN-*co*-PAA_{nfm} configuration.

It appears that the peak currents were proportional to the square roots of scan rates ($\nu^{1/2}$) for the both electrodes, in the range of 5−2000 mV s^{-1} (as shown in parts C and D of Figure 2). The linearity of i_p against $\nu^{1/2}$ plot seems to indicate that the redox behavior at the electrodes is diffusion controlled. For the PAN-*co*-PAA coating, this effect may be ascribed to a hindered diffusion of counterions within the nanopores of this deposit, the latter being necessary for counterbalancing the oxidation of Ru(II) into Ru(III) complex.

ECL Behavior. The ECL behaviors of $[Ru(bpy)_3]^{2+}$ incorporated into PAN-*co*-PAA_{nfm} and PAN-*co*-PAA coating have been studied with TPA as a representative coreactant, since the $[Ru(bpy)_3]^{2+}$/TPA system has been fully investigated and gives a stronger ECL efficiency.[13] Figure 5 depicts the corresponding CVs and ECL behaviors of the $[Ru(bpy)_3]^{2+}$-electrodes modified by PAN-*co*-PAA_{nfm} (curve a) and PAN-*co*-PAA coating (curve b) in 0.1 M PBS (pH 7.0) containing 1.0×10^{-4} M TPA. Compared with the CVs performed in the absence of TPA at the same scan rate (100 mV s^{-1} in Figure 4), a dramatic increase in the oxidation current combined with a simultaneous decrease of the reduction current demonstrate the electrocatalytic oxidation of TPA by the above-mentioned electrode (Figure 5A). These results indicate that the $[Ru(bpy)_3]^{2+}$ was incorporated onto the electrodes and retained its electroactivity. For the $[Ru(bpy)_3]^{2+}$/PAN-*co*-PAA_{nfm}/GCE, the first oxidation peak current at ~0.75 V is due to the direct oxidation of TPA,[16−18] while the second oxidation current peak was ascribed to the electrocatalytic oxidation of TPA by the electrogenerated $[Ru(bpy)_3]^{3+}$. This signal appears at ~0.9 V and reaches its maximum value (12.3 μA) at 1.1 V (Figure 5A, curve a). In contrast, the CV of $[Ru(bpy)_3]^{2+}$/PAN-*co*-PAA/GCE shows only the electrocatalytic oxidation of TPA, no direct oxidation of TPA occurring at the electrode surface (Figure 5A, curve b). This illustrates the markedly less porous of the $[Ru(bpy)_3]^{2+}$/PAN-*co*-PAA/GCE compared to the nanofibers-modified electrode. It should be noted that the comparison of the cyclic voltammograms of a more concentrated TPA solution (0.01 M) recorded at PAN-*co*-PAA and PAN-*co*-PAA_{nfm} electrodes clearly shows that PAN-*co*-PAA coating, contrarily to PAN-*co*-PAA_{nfm} deposit, prevented the electrochemical oxidation of TPA (Figure 5A, inset).

The direct oxidation of TPA at electrode plays an important role in the ECL process of the $[Ru(bpy)_3]^{2+}$/TPA system.[16] The comparison of the ECL intensity−potential curves clearly shows that the ECL emission obviously increases with the PAN-*co*-PAA_{nfm} modified electrode (Figure 5B). The ECL intensity at the PAN-*co*-PAA_{nfm} modified electrode is more than 100-fold that obtained from the PAN-*co*-PAA deposited film modified electrode. Moreover, its onset of luminescence occurred near 0.94 V, and then the ECL intensity rises steeply until it reaches a maximum near 1.2 V, which is consistent with the oxidation potential of $[Ru(bpy)_3]^{2+}$ (Figure 5B, curve a). The ECL reaction of the $[Ru(bpy)_3]^{2+}$/TPA system can be expressed as the following equations[19]

$$[Ru(bpy)_3]^{2+} - e^- \rightarrow [Ru(bpy)_3]^{3+} \quad (1)$$

$$TPAH^+ - H^+ \rightarrow TPA \quad (2)$$

$$TPA - e^- \rightarrow TPA^{\bullet+} \quad (3)$$

$$TPA^{\bullet+} - H^+ \rightarrow TPA^{\bullet} \quad (4)$$

$$[Ru(bpy)_3]^{3+} + TPA^{\bullet} \rightarrow [Ru(bpy)_3]^{2+*} \quad (5a)$$

$$[Ru(bpy)_3]^{3+} + TPA \rightarrow [Ru(bpy)_3]^{2+*} + TPA^{\bullet+} \quad (5b)$$

$$[Ru(bpy)_3]^{2+*} \rightarrow [Ru(bpy)_3]^{2+} + h\nu\ (610\ nm) \quad (6)$$

The dramatically enhanced ECL of $[Ru(bpy)_3]^{2+}$/PAN-*co*-PAA_{nfm}/GCE may arise from the following factors: (1) The nanosized PAN-*co*-PAA fibers can preserve the accessibility to the electrode surface (2) The PAN-*co*-PAA_{nfm} offers an open porous structure, which allows an easy permeation of the coreactant TPA and a good accessibility to the immobilized ruthenium complexes. TPA can thus be directly oxidized at the electrode surface and can react efficiently with electrogenerated $[Ru(bpy)_3]^{3+}$.

(16) Jiang, P.; Yan, L.; Liu, Y. H.; Yuan, H. Y.; Xiao, D. *Electroanalysis* **2009**, *21*, 1611–1616.
(17) Zu, Y. B.; Bard, A. J. *Anal. Chem.* **2000**, *72*, 3223–3232.
(18) Wang, H. Y.; Zhang, X. L.; Tan, Z. A.; Yao, W.; Wang, L. *Electrochem. Commun.* **2008**, *10*, 170–174.
(19) Miao, W.; Choi, J.-P.; Bard, A. J. *J. Am. Chem. Soc.* **2002**, *124*, 14478–14485.

Table 1. Comparison of ECL Intensities to Seven Analytes in Aqueous Solution

coreactant	ECL intensity/A.U. $[Ru(bpy)_3]^{2+}$/PAN-*co*-PAA/GCE	ECL intensity/A.U. $[Ru(bpy)_3]^{2+}$/PAN-*co*-PAA_{nfm}/GCE	amplification factor
TPA (1×10^{-4} M)	5.05	510.1	101
NADH (1×10^{-4} M)	1.68	102.14	60.8
$C_2O_4^{2-}$ (1×10^{-3} M)	3.79	176.24	46.5
ofloxacin (1×10^{-4} M)	2.53	221.70	87.6
gentamycin (1×10^{-4} M)	1.47	116.28	79.1
tetracycline (1×10^{-4} M)	1.12	88.44	79.0
proline (1×10^{-4} M)	0.84	65.21	77.6

In addition, the proposed PAN-*co*-PAA_{nfm} modified electrode exhibits also the superior performance to other analytes in aqueous solution. As summarized in Table 1, the amplification factors for the ECL intensities to NADH (1×10^{-4} M), $C_2O_4^{2-}$ (1×10^{-3} M), ofloxacin (1×10^{-4} M), gentamycin (1×10^{-4} M), tetracycline (1×10^{-4} M), and praline (1×10^{-4} M) are 60.8, 46.5, 87.6, 79.1, 79, and 77.6, respectively.

CONCLUSIONS

In summary, we demonstrated that the electrospinning approach allows depositing large amounts of polymer to the electrode while maintaining accessibility to the electrode surface. The specific properties of the polymer material, in this case the electrostatic interactions, can be exploited and combined with electrochemical processes. Electrospun nanofibers present specific properties such as large surface area-to-volume ratio and huge active sites for further interaction or attachment. Thus, electronspun nanofibers can be used as the attractive host matrix for the available loading of guest molecules in the electrode modification. Moreover, the target molecules can penetrate freely into the matrix and react with the immobilized guest molecules and result in the enhanced response due to the porous structure of the electrospun nanofibrous mat.

ACKNOWLEDGMENT

This project was supported by the National Nature Sciences Foundation of China (Grants 20905011, 20773108, and 20810102052) and the University science research project of Jiangsu province (Grant 09KJB150015).

Received for review February 17, 2010. Accepted June 7, 2010.

AC100435Z